AuS and SH Bond Formation/Breaking during the Formation of Alkanethiol SAMs on Au(111): A Theoretical Study

Frederik Tielens*,† and Elizabeth Santos*,‡

UPMC Univ Paris 06, UMR 7197, and CNRS, UMR 7197, Laboratoire de Réactivité de Surface, Tour 54-55, 1 étage - Casier 178, 4, Place Jussieu, F-75005 Paris, France, Institut für Theoretische Chemie, Universität Ulm, Albert-Einstein-Alée 11, D-89081 Ulm, Germany, and Instituto de Física Enrique Gaviola (IFEG), Universidad Nacional de Córdoba - CONICET, Argentina

Received: March 6, 2010; Revised Manuscript Received: April 12, 2010

The bonding of propanethiol molecules on a Au(111) surface is investigated using period DFT calculations within the framework of our model for chemical bond breaking that was recently proposed. The S−H bond breaking and the Au−S bond formation are analyzed through the evolution of the density of states. The energetics confirms the complexity of the reaction emerging from the interthiol chain interaction. The formation of a self-assembled monolayer is explained through a two-step mechanism, S−H bond breaking and Au−S bond formation. The production of H_2 is found to be more favorable than the formation of Au−H species. The bonding and antibonding electronic states of the S−H bond have been identified and their evolutions during the process of bond breaking carefully analyzed. The corresponding bonding and antibonding states for the C−S bond are practically not affected during this process, indicating that the bond is preserved. The s orbital of the hydrogen atom strongly interacts with the gold surface and finally a Au−H bond is formed.

Introduction

When molecules adsorb at surfaces at high enough coverages, they tend to arrange and make adsorption patterns, or so-called self-assembled monolayers (SAM), that are ruled by their intermolecular forces. Examples of SAMs on solid surfaces are thiols, silanes, and phosphonates.[1,2] A specific linker is used to guide the self-assembly process on each type of substrate. Among the most popular SAMs, because of both their promising and current applications in several fields of nanotechnology, are alkanethiol (and alkanedithiol) monolayers on metals and metallic nanoparticles (particularly Au).[3]

Since alkanethiol SAMs represent an easy path to link bio-organic molecules,[4] they are essential in many methods to build a variety of devices and materials.

A recent approach to investigate the reaction pathways for methanethiol adsorption on Au(111) has been given by Lustemberg et al.[5] They found a molecular adsorbed state without the breaking of the S−H bond with the sulfur atom on top sites and the hydrogen near a bridge site. They have also shown that the dissociation process is energetically less favorable with an activation energy of about 0.4 eV. Andreoni et al.[6] have also considered both dissociative and molecular configurations of methanethiol and found that the dissociated species can coexist with the adsorbed "intact" species and become favored if accompanied by the formation of molecular hydrogen. They have also performed Mulliken population analysis indicating that the adsorbate has a net excess charge of about 0.3e in comparison with the free radical charge. Other questions concerning the binding of thiols at Au(111) is the desorption mechanism, on which one cannot give yet a clear-cut answer. Some authors predict no C−S nor S−H bond breaking upon adsorption,[7] and others a recombination with an H[8] or the formation of disulfides.[9]

The formation of SAMs of alkanethiols on a gold (111) surface has been studied for several decades.[3,10,11] In particular, studies exist on its electronic structure to investigate the covalent S−Au bond.[12−15] Most of these type of investigations have been carried out on sulfur, H_2S, methanethiol, or amino acids such as cysteine and others. Interesting contributions are those of Di Felice et al.[16,17] where the electronic structure of different configurations of SAMs on Au(111) obtained from the adsorption of cysteine and cystine is analyzed, with a focus on the total and projected density of states on gold, sulfur, and the carbon bonded to the sulfur. The detailed character of the electronic states at the interface is also discussed. States near the Fermi level are found to have a metal−molecule antibonding character, whereas metal−molecule bonding states appear near the lower edge of the d band of gold.

On the molecular level one starts to have a description of the adsorption site and geometry at high coverage of thiols on Au(111) surfaces.[14,18−21] Nevertheless, the first steps in the reaction of formation of the layer, i.e., the initial binding mechanism of the thiol with Au, are still under debate. Indeed, does the thiol physisorb or chemisorb? In other words, does the S−H bond of the thiol dissociate upon interaction with the surface? And, if so, what happens with the hydrogen atom after the formation of the S−Au bond? Does the hydrogen recombines with another hydrogen atom in the neighborhood, or does it stay adsorbed at the Au surface? In summary, many questions are still unanswered concerning the formation mechanism of thiol layers.

In this work we present an ab initio investigation on the formation of propanethiol on Au. We combine DFT calculations with the theory for bond breaking recently developed in our group.[22−25]

The thiol chosen as the model is propanethiol because it has the property to be large enough to be considered as a potential initiator of experimentally used thiols forming SAMs, and small

† Laboratoire de Réactivité de Surface.
‡ Universität Ulm and Universidad Nacional de Córdoba.

10.1021/jp102036r
Published on Web 05/05/2010

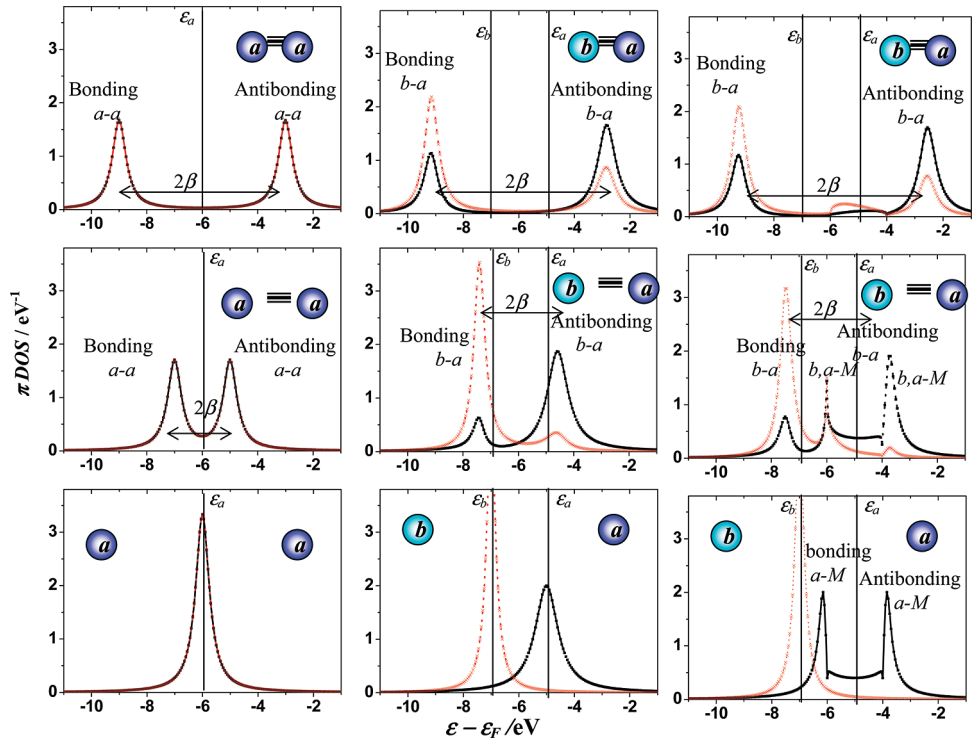

Figure 1. Distribution of DOS, ρ_a and ρ_b, for both orbitals of the atoms forming a molecule, when it is close to the metal surface. First column: the process of dissociation for a homonuclear molecule when both atoms are at equivalent positions (same distance to the surface). Second and third columns: the process of dissociation for a heteronuclear molecule (or a homonuclear molecular with the atoms at different distances to the surface). Top: equilibrium condition for the molecule, $\beta = -3$ eV. Middle: elongation of the bond a−a (or a−b), $\beta = -1$ eV. Bottom: molecule completely dissociated in 2a (or a + b), $\beta = 0$ eV. Parameters used for the calculations: (first column) $\varepsilon_a = -6$ eV, $\Delta_a = 0.3$ eV = constant, $\Lambda_a = 0$, $\beta = -3$ eV; (second and third columns) $\varepsilon_a = -5$ eV, $\varepsilon_b = -7$ eV, (●, black) ρ_a, (×, red) ρ_b. In the second and third columns, two different electronic structures for the metal are considered: (second column) a constant distribution of electronic states with $\Delta_a = 0.5$ eV = constant, $\Delta_b = 0.2$ eV = constant, $\Lambda_{a,b} = 0$; (third column) a superposition to the constant structure of a semielliptical band of width $w = 1$ eV centered at $\varepsilon_c = -5$ eV (it is assumed that only the atom a interacts with this band, with a coupling constant of $|V_a|^2 = 2$ eV^2).

enough to perform state-of-the-art periodic DFT calculations on the system.

In the past, model calculations on alkanethiol SAMs have been performed in our group[26−28] in line with present research topic. The aim of this work is to present a detailed electronic structure investigation of the formation/breaking of S−H and S−Au bonds in the context of alkanethiol SAMs

Theory and Computational Details

a. Model. Propanethiol is adsorbed on a Au(111) surface. The initial geometry was built from the one obtained in our former study on undecanethiol SAMs, which agrees with the results found in other studies.[27]

It was found that the thiols adsorb on different possible sites simultaneously, forming unit cells containing up to four thiol chains. Our group showed on the ab initio level backed up with IR and XPS experiments that at least two adsorption sites are present in the same unit cell.[29]

Nevertheless, the energy differences between the different adsorption configurations are very small, and one can approximate the SAMs of thiols on the Au(111) surface being adsorbed on the same type of site, namely, the bridge-like site somewhere between the hollow hpc or fcc and the bridge site.

In summary, since we will concentrate on the S−H bond cleavage and S−Au bond formation, our model will consist of the simple $(\sqrt{3} \times \sqrt{3})$R30° unit cell containing one thiol chain; unless mentioned, double $(2\sqrt{3} \times \sqrt{3})$R30° and quadruple $(2\sqrt{3} \times 2\sqrt{3})$R30° cells will be used.

The Au(111) surface is modeled using a slab containing five layers with the two bottom ones fixed to the bulk positions.[26,27,30,31] The cell parameters are obtained after optimization of the bulk at the same level of calculation as the thiol SAM.

The geometry optimization and minimization of the total energy are performed using the VASP code.[32,33] In the periodic density functional theory framework used, the Kohn−Sham equations are solved by means of the revised Perdew−Burke−Ernzerhof (PPBE) functional.[34−37] The electron−ion interaction is described by the projector augmented-wave method (PAW).[38,39]

The atom positions of the thiol together with the upper three layers are relaxed without geometrical constraints. Optimizations are performed at a 5 × 5 × 1 *k*-point mesh for the Brillouin-zone integration with an energy cutoff of 500 eV, a level off calculation at which the energies are converged within 0.05 eV.

The electronic properties such as the density of states (DOS) are calculated by performing a single-point calculation at higher precision (11 × 11 × 1 *k*-point mesh) than the geometry optimization calculations.

b. Theoretical Description. According to the model of Anderson−Newns[40,41] for adsorption on metal surfaces, the projected DOS for the atomic orbitals corresponding to the reactant is given by the following expression:

$$\rho_a(\varepsilon) = \frac{1}{\pi} \frac{\Delta(\varepsilon)}{[\varepsilon - \varepsilon_a - \Lambda(\varepsilon)]^2 + \Delta^2(\varepsilon)} \qquad (1)$$

where "a" symbolizes atom a with an energy level ε_a for the isolated atom and $\Delta(\varepsilon)$ and $\Lambda(\varepsilon)$ are the *chemisorption functions* that describe the quantum-mechanical coupling of the a atom to the metal. They are interconnected through a Hilbert transform[40,41] and produce a broadening (Δ) and a shift (Λ) of

the atomic energy levels. They are directly related to the electronic density of states of the metal and usually decrease almost exponentially with the distance of the reactant to the metal. Recently, we have extended this model for adsorption processes with simultaneous bond breaking.[23,25] This model is general and can also be applied to processes occurring in an electrochemical environment, where electron transfer processes can take place.

Assuming the simplest Hückel approximation for the interaction between the atoms forming the molecule, the expression (eq 1) for the density of states of a homonuclear molecule with both atoms in equivalent positions becomes

$$\rho_{aa}(\varepsilon) = \frac{\Delta(\varepsilon)}{\pi}\left[\frac{1}{[\varepsilon - \varepsilon_a - \Lambda(\varepsilon) + \beta]^2 + \Delta^2(\varepsilon)} + \frac{1}{[\varepsilon - \varepsilon_a - \Lambda(\varepsilon) - \beta]^2 + \Delta^2(\varepsilon)}\right] \quad (2)$$

with β being an attractive parameter directly related to the bonding energy of the molecule which is the off-diagonal element of the secular determinant. The first term in eq 2 represents a bonding, while the second one represents an antibonding state between the atoms. If the interaction with the electronic states of the metal is weak, Δ is small and can be considered constant and Λ is consequently zero. This is a typical behavior for the interaction with sp bands, which are wide and structureless. In this case, the distribution of electronic states of the molecule has the form of two Lorentzians centered at ε_a and separated by 2β. Figure 1, at the left, shows the distribution of density of states for both orbitals of the atoms forming the molecule. Both atoms are equivalent and the corresponding DOS are identical. The result for a hypothetical molecule at its equilibrium configuration is shown on the top of Figure 1.

Within the Hückel approximation and without spin interactions, $-\beta$ is half of the dissociation energy. During the process of dissociation, the magnitude of β becomes smaller (the interactions between the atoms decreases with the separation distance) and both states, bonding and antibonding, approach each other (Figure 1, middle) until they converge in a unique peak (Figure 1, bottom). For a heteronuclear molecule the expression of the density of states ($\rho_{ab} = \rho_a + \rho_b$) is more complicated since it contains the energy levels of the atomic orbitals participating in the bond ε_a and ε_b, and their corresponding interaction constants with the metal $\Delta_{a,b}$ and $\Lambda_{a,b}$, which can be different for each atom. However, the bonding and antibonding states still can be distinguished (see Figure 1, on right). Because of the different positions of the atomic orbitals a and b, the bond is no longer covalent and is now polarized. Thus, in the example shown in Figure 1, the electronic density of orbital b, which lies deeper in energy, is higher than that of a at the bonding state, which is at higher energies. The opposite happens at the corresponding antibonding state. When the molecule completely dissociates, two peaks are observed corresponding to the individual atomic orbitals centered at ε_a and ε_b, respectively (Figure 1 right, bottom). Additionally, if the interaction with the metal is strong enough, a splitting of each state can occur into bonding and antibonding, but now between the atom and the metal as illustrated at the final state of the dissociation of the heteromolecule (see dashed line in Figure 1, third column, bottom). It is interesting to observe that the orbital with the weaker interaction with the metal is also indirectly affected by the stronger interaction of the other orbital through the bond with that atom. In the middle plot (Figure 1) on the right side third column, the antibonding states of the

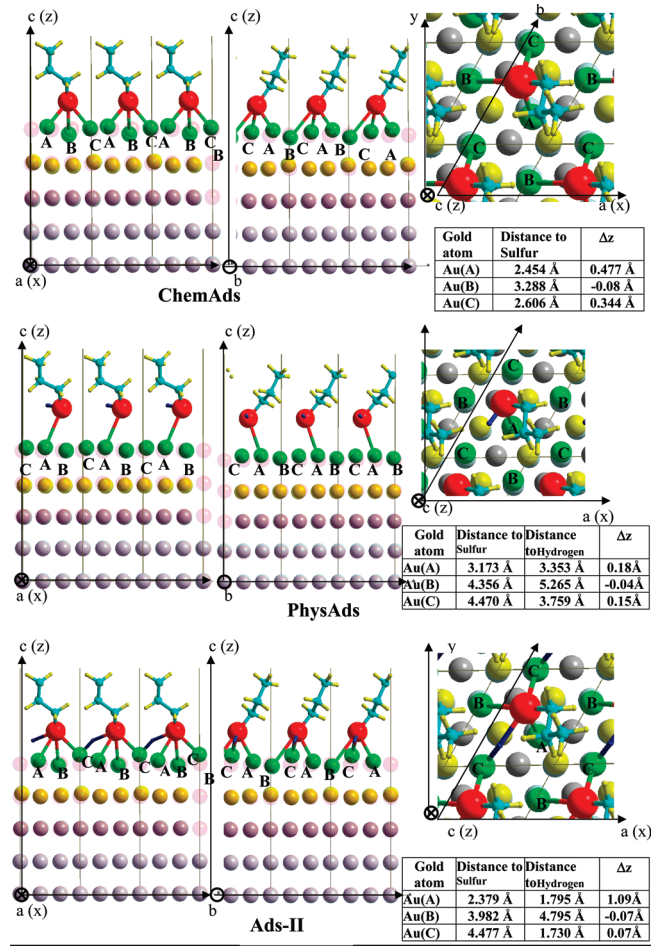

Gold atom	Distance to Sulfur	Δz
Au(A)	2.454 Å	0.477 Å
Au(B)	3.288 Å	-0.08 Å
Au(C)	2.606 Å	0.344 Å

Gold atom	Distance to Sulfur	Distance to Hydrogen	Δz
Au(A)	3.173 Å	3.353 Å	0.18Å
Au(B)	4.356 Å	5.265 Å	-0.04Å
Au(C)	4.470 Å	3.759 Å	0.15Å

Gold atom	Distance to Sulfur	Distance to Hydrogen	Δz
Au(A)	2.379 Å	1.795 Å	1.09Å
Au(B)	3.982 Å	4.795 Å	-0.07Å
Au(C)	4.477 Å	1.730 Å	0.07Å

Figure 2. Model for the chemisorbed, physisorbed propanethiol and SAM where the hydrogen atom is also adsorbed (side and top views). The distances between the atoms are also given as well the displacement Δz of the gold atoms from their original equilibrium positions,

atom b show a splitting although Δ_b is small. This effect of tuning the through-bond interaction in a two-center problem has been extensively discussed by Levstein and Pastawski[42,43] and is a general phenomenon in electron quantum transport. Strong interactions with the metal can particularly be observed when one orbital of the molecule coincides in the energy range with the location of a d band. However, this type of interaction has a shorter domain and the electrons are more localized. This catalytic effect is important during adsorption processes where the reactant approaches the metal.[25]

The position of the electronic states of the molecule on the energy scale depends on a series of parameters, then, one has to consider an effective $\tilde{\varepsilon}_i$:

$$\tilde{\varepsilon}_i = \varepsilon_i^o - 2\lambda q + e_o\eta + \text{o.t.} \quad (3)$$

with ε_i^o being the position of the atomic orbital i when the atom is isolated. The second term takes into account the fluctuation produced by the interaction with the solvent, λ being the reorganization energy according to the model of Marcus and Hush[44,45] and q the corresponding solvent coordinate. This term is particularly important for charged species where the solvation is strong. In an electrochemical environment, the position of the electronic states of the reactant can also be shifted relative to the Fermi level of the metal electrode by varying the potential η applied at the interface. This term accounts for electron transfers (oxidation/reduction reactions). The last term o.t. contains other contributions, such as interactions of opposite

TABLE 1: Binding Energies of Methane- and Propanethiol and -thiolate Radicals with a Au(111) Surface (Energies in eV)

unit cell	$2\sqrt{3} \times 2\sqrt{3}$ 25% ML	$\sqrt{3} \times \sqrt{3}$ 1 ML	$2\sqrt{3} \times \sqrt{3}$ 1 ML	$2\sqrt{3} \times 2\sqrt{3}$ 1 ML	lit. data exp	lit. data theoretical
methanethiol	−0.49			−0.11	−0.5[47]	−0.5[14,52] −0.22 to −0.66[9]
methanethiolate	−1.90			−1.37	−1.73[10]	−1.7[49]
propanethiol	−0.47	0.02	−0.08	−0.11	−0.60[47]	
propanethiolate	−1.83	−1.29	−1.20	−1.35	−1.30[47]	−1.64[48] to −1.81

spins, image and dipole effects, overlapping between orbitals, and exchange correlations that can be obtained from DFT calculations.

In the examples shown in Figure 1 both bonding and antibonding states lie in all the cases below the Fermi level. Thus, the molecules a−a and b−a are not stable at the interface of that metal and the dissociation reaction should occur spontaneously because both bonding and antibonding orbitals are occupied. The shift of the orbitals' positions by fluctuations of the solvent configuration or by applying a potential at the interface (second and third terms of eq 3) plays a key role in facilitating a dissociation reaction or an electrochemical reaction (oxidation/reduction). For example, the oxidation of hydrogen is possible because of the stabilization of the proton by solvation.[24]

Results and Discussion

a. Geometry. The geometry of propanethiolate radical chemisorbed on the Au(111) surface forming a monolayer is shown in Figure 2, top. Important parameters are the adsorption site and the S−Au distance. The thiol is found to adsorb at a displaced bridge site, in agreement with former experimental and theoretical findings.[27] The shortest S−Au bond distance is 2.45 Å. The configuration of the molecule (distances and angles between the different atoms) practically does not change in comparison with the isolated molecule's configuration. Only the distance between the sulfur and the next carbon is slightly elongated (about 3−4%). An important perturbation of the position of the gold atoms is observed. They are displaced from their original equilibrium positions when the adsorbate was absent. This effect extends up to the second underlayer, as can be observed from the Figure 2, top, where the gold atoms in the slab without the adsorbate are shown in the background as shadows. This wavelike shape of the gold atom position at the surface has been also found in other studies with methanethiol.[17,46]

The physisorption of the propanethiol molecule on the Au(111) surface has a different adsorption site, compared with that for the chemisorbed species (Figure 2, middle). The propanethiol molecule is found to adsorb on an off-center atop site with a distance from the surface's Au atom of 3.173 Å. Here the perturbation on the position of the gold atoms is less, but still noticeable.

The formation of the Au−S bond is studied by varying the Au−S distance between the physisorbed and the chemisorbed species. In a first stage the position of the S atom was frozen in the *xy*-plane, keeping the atom free to relax in the *z* direction for a series of S−H distances, since the strengthening of the S−Au bond is expected to weaken the S−H bond. The mean observation of this series of optimizations is that the adsorption geometry does not change for a large range of S−H distances. Indeed, geometry close to chemisorption is only found for distances larger than 2.3 Å. Interesting to note, despite the geometry constraints, the H atom is adsorbed at a bridge position between the Au(A−C) atoms to the gold surface without any energy barrier (Figure 2, bottom). For this geometrical configuration, the gold atom called "C", which is involved in both the bonds with the sulfur and with the hydrogen atom, is relatively far from its original position.

b. Energy Profile: Possible Reaction Path for the Formation of Chemisorbed Species. To compare our results with literature data, we have investigated the energetics of methanethiol on Au(111): We have first performed calculations for methanethiol and the methanethiolate radical since most studies on thiol SAMs are performed using these molecules for model. The adsorption energies are tabulated and compared with experimental and theoretical results from the literature in Table 1.

The adsorption energies of propanethiol on Au(111) are calculated as follows:

Physisorption.

$$C_3H_7{-}SH + Au(slab) \rightarrow C_3H_7{-}SH...Au(slab) \quad (4)$$

The obtained energy for this reaction was −0.11 eV (exothermic). It is obvious that this value is very small and thus difficult to confirm experimentally. This result was obtained using a $2\sqrt{3} \times 2\sqrt{3}$ unit cell. Experimental values of about −0.60 eV are found,[47] which are not in agreement with the theory. The reason for this difference is probably due to the fact that dispersion is not included in the methodology used or that the model used is not a good representation of the adsorption site. Moreover, this model represents a monolayer configuration, in which the chains interact with each other and the dispersion and steric forces are maximal. The physisorption energy for a 25% monolayer is found to be −0.47 eV, which is a more reasonable result. The adsorption energy is thus clearly dependent on the surface coverage.

Experimentally, it is still unclear if thiol SAMs are formed by thiols or thiolate radicals after cleavage of the S−H bond. In the latter case, hydrogen could either stick to gold or desorb in molecular form. No evidence of either process is generally found.

Chemisorption.

$$C_3H_7S + Au(slab) \rightarrow C_3H_7S{-}Au(slab) \quad (5)$$

In the case that a $2\sqrt{3} \times 2\sqrt{3}$ unit cell containing four thiolate radicals (full monolayer) is used, we have obtained an energy value associated with this reaction of −1.35 eV. For a 25% monolayer a chemisorption energy of −1.83 eV is calculated in agreement with former theoretical calculations obtained on different unit cells using geometrically constraint models, where values between −1.64 eV[48] and −1.81 eV[14] are reported.

Experimentally, an adsorption (chemisorption) energy of −1.30 eV[47] is found, which is in very good agreement with our calculations. This result is clearly due to canceling of errors, since the contribution due to dispersion, which can be approximated to be 0.15 eV, is not considered in the DFT method used.

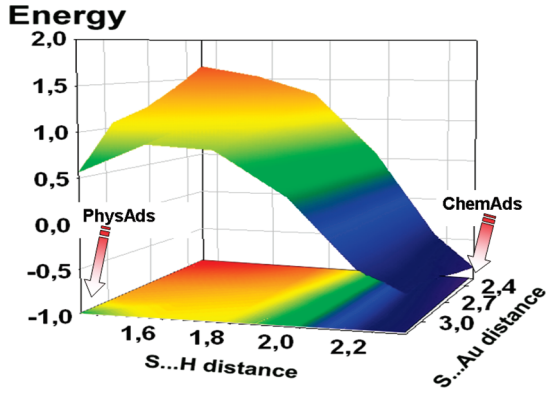

Figure 3. Potential energy surface of propanethiol adsorption on Au(111). Distances in Å and energies in eV).

With both physi- and chemisorption energies one can evaluate the energy associated with the surface reactions occurring during SAM growth. It should be noted that this reaction energy ΔE_r is calculated with respect to the RS radical. So, if one considers a more realistic reaction scheme such as

$$R{-}SH \rightarrow R{-}S^{\bullet} + H^{\bullet} \qquad \Delta E_r = 3.73\ \text{eV} \qquad (6)$$

$$H \rightarrow {}^1/_2H_2 \qquad \Delta E_r = -2.27\ \text{eV} \qquad (7)$$

$$R{-}S^{\bullet} + \text{Au(slab)} \rightarrow R{-}\text{SAu(slab)} \qquad \Delta E_r = -1.35\ \text{eV} \qquad (8)$$

$$\text{Total:} \quad R{-}SH + \text{Au(slab)} \rightarrow R{-}\text{SAu(slab)} + {}^1/_2H_2 \qquad \Delta E_r = 0.11\ \text{eV} \qquad (9)$$

and

$$R{-}SH \rightarrow R{-}S^{\bullet} + H^{\bullet} \qquad \Delta E_r = 3.73\ \text{eV} \qquad (10)$$

$$H^{\bullet} \rightarrow H_{ads}\ \text{on Au} \qquad \Delta E_r = -1.88\ \text{eV} \qquad (11)$$

$$R{-}S^{\bullet} + \text{Au(slab)} \rightarrow R{-}\text{SAu(slab)} \qquad \Delta E_r = -1.35\ \text{eV} \qquad (12)$$

$$\text{Total:} \quad R{-}SH + \text{Au(slab)} \rightarrow R{-}\text{SAu(slab)} + H_{ads} \qquad \Delta E_r = 0.50\ \text{eV} \qquad (13)$$

one obtains a more realist view on the energetics involved.

The chemisorption reaction when a H_2 molecule is formed is found to be slightly endothermic by about 0.10 eV, and 0.50 eV when the hydrogen atom is adsorbed to the Au(111) surface. The elementary step of binding the propanethiol radical is exothermic (−1.35 eV). Both reactions are calculated to be endothermic, which was also found by Gottschalck et al.[49] for the methanethiolate radical. They invoked the possibility of a disproportionation reaction leading to H_2S and CH_4 yielding an exothermic reaction energy, and/or the reconstruction of the gold surface. The latter effect was considered in our calculations but did not change the thermodynamics. Here again it is expected that the steric hindering between the chains is the limiting factor; indeed the model represents a complete monolayer, with the thiol molecules interacting with each other.

The interaction energy calculated for a 25% monolayer is −1.83 eV, yielding a reaction energy of −0.37 and +0.02 eV for the H_2 formation (eq 9) and H adsorption reactions (eq 13), respectively. In other words, SAM growth is indeed thermodynamically favorable, especially when H_2 is formed, at low surface coverage rates, and the more the SAM grows, the less thermodynamically favorable becomes the reaction.

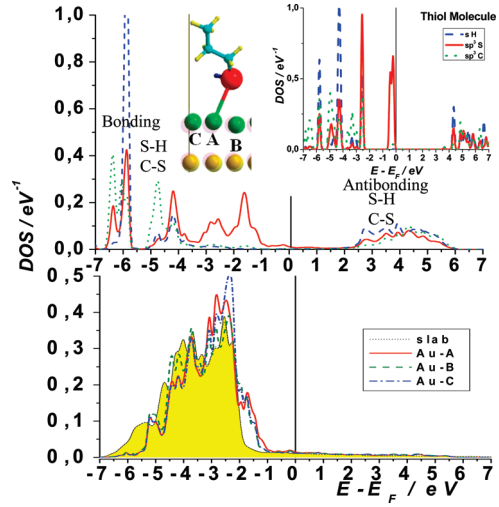

Figure 4. Top: projected DOS on the sulfur s−p orbitals (full line, red), on the carbon bonded to the sulfur s−p orbitals (dotted line, green), and on the hydrogen of the thiol group s orbital (dashed line, blue) for the physisorbed species shown in Figure 2-top. In the inset are shown the corresponding DOS for the propanethiol molecule far away from the gold surface. Bottom: projected DOS on the d bands of the three different gold atoms called A, B, and C. The curve with the filled surface corresponds to the gold atoms of the surface in absence of any adsorbate.

The potential energy surface of propanethiol is constructed as a function of the Au−S and the S−H distance (Figure 3). To obtain reasonable minima and maxima, because of the formation of a H atom (energetically unfavorable reaction), a second H atom was modeled by adding an empirical Lennard-Jones potential having a minimum corresponding to the formation of a H_2 molecule at 2.3 Å. From this plot one can obtain a first approximation of the energy barrier for the S−H bond breaking and the reaction path for the formation of the chemisorbed species.

It is found that the chemisorption reaction occurs in two steps: (1) the breaking of the S−H bond, with a barrier of 0.32 eV (approximated) followed by (2) a barrierless binding of the RS radical to the gold surface, which is in agreement with the experimentally proposed values.[50]

c. Electronic Structure. The interpretation of the electronic structure of the system investigated in this work is complicated because of the several chemical bonds present in the propanethiol molecule. There are different possibilities for hybridization in the molecule, and the interaction of the reactant with the different bands of the gold surface can be complex. However, we will try to describe the system in the framework of the model proposed previously[23,25] and discussed above. We focus on the possibility of breaking the sulfur−hydrogen bond and analyze in detail the changes in the electronic density of states of the atoms that are closest to the metal: the sulfur, the hydrogen of the thiol group, and the carbon bonded to the sulfur. The projected density of states on the s and p states of these atoms is investigated. Finally, the gold atoms labeled A, B, and C in Figure 2 are considered, and the d orbital components at the different spatial directions (d_{xy}, d_{xz}, d_{yz}, $d_{x^2-y^2}$, and d_{z^2}) are examined.

Figure 4 shows the results obtained for the geometric configuration called "PhysAds" which has been discussed in the previous sections. The full red line shows the DOS corresponding to the sulfur atom, the dotted green line to the carbon atom bonded to the sulfur and the dashed blue line to the hydrogen atom of the thiol group. A multiplicity of peaks

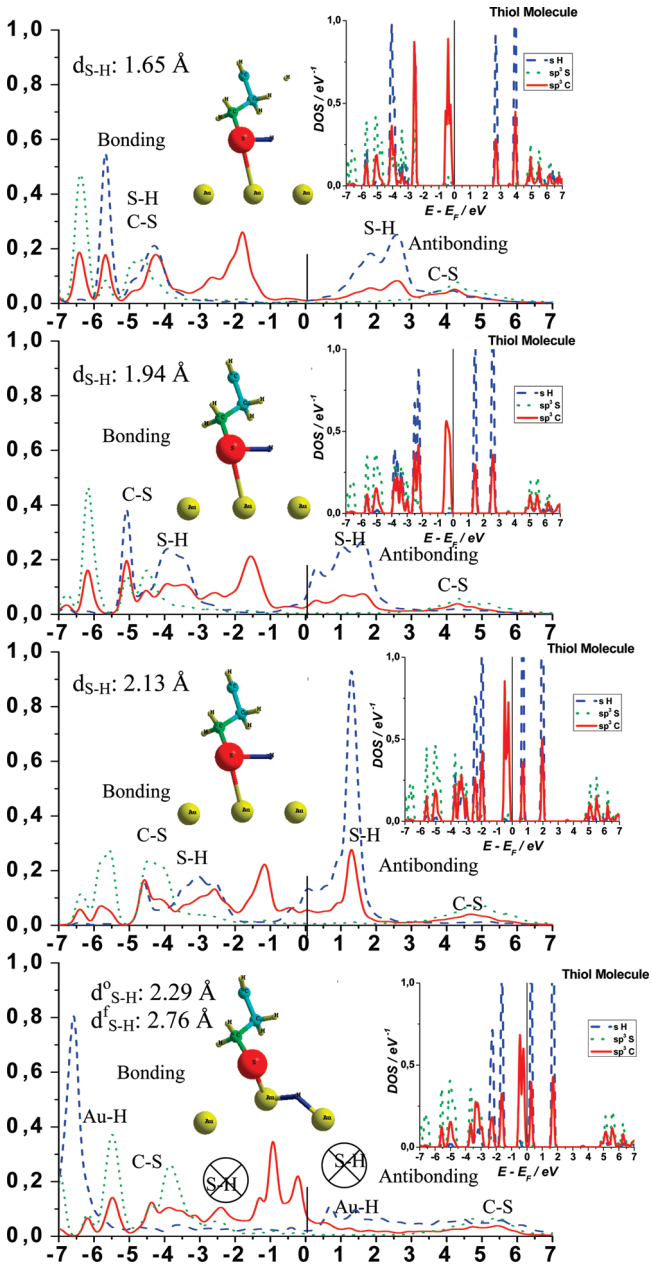

Figure 5. Projected DOS on the sulfur s−p orbitals (full line, red), on the carbon bonded to the sulfur s−p orbitals (dotted line, green), and on the hydrogen of the thiol group s orbital (dashed line, blue) for the physisorbed species shown in Figure 2-top during the elongation of the S−H bond. In the inset are shown the corresponding DOS for the propanethiol molecule far away from the gold surface.

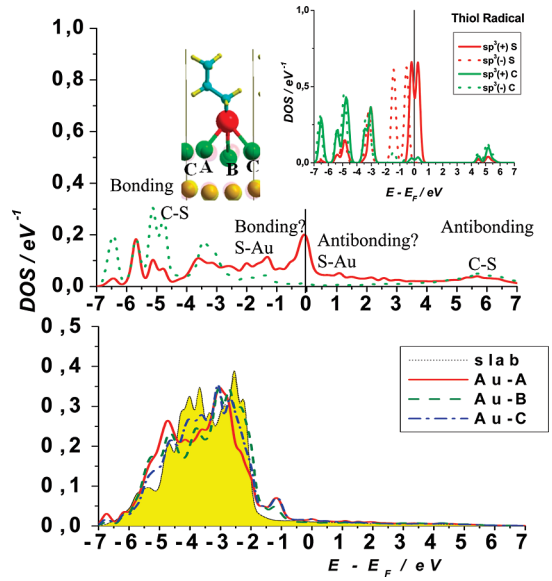

Figure 6. Top: projected DOS on the sulfur s−p orbitals (full line, red), and on the carbon bonded to the sulfur s−p orbitals (dotted line, green) for the chemisorbed species shown in Figure 2-middle. In the inset are shown the corresponding DOS for the two spins of the propanethiol radical far away from the gold surface. Bottom: projected DOS on the d bands of the three different gold atoms called A, B, and C. The curve with the filled surface corresponds to the gold atoms of the surface in absence of any adsorbate.

can be observed due to the participation of several orbitals in the bonds. However, one can distinguish two different groups, which can be identified as bonding and antibonding states. The corresponding DOS for the propanethiol molecule at long distances from the gold surface is shown for comparison in the inset. A shift to lower energies and a broadening of the electronic states caused by the interaction with the gold surface is also noticed. This last effect occurs especially for those states lying in the energy range between −5 and −1 eV, where the d band of gold appears. The two peaks appearing at −4.7 and −4.2 eV in the molecule far away from the surface only move to −6.4 and −5.9 eV, respectively, when the molecule is at the surface without broadening or changing their shapes. They can be assigned to bonding states between the sulfur with the carbon and with the hydrogen. The other group of bonding state peaks, where also overlap between the states of sulfur, carbon, and hydrogen occurs, shifts from the energy interval between −4 and −3 eV into the range −5 and −3.5 eV. The strong broadening of the original peak of the molecule at −2.7 eV is noticeable. This peak and the states of sulfur at the gold surface between −3 and −1 eV do not show any overlap either with carbon or with the hydrogen state. The region above −2 eV is expected to correspond to the lone electron pair, which does not participate in the bonding with those atoms. These states appear in the isolated molecule between −1 and 0 eV. At energies above the Fermi level, the corresponding antibonding states for C−S and S−H can be observed. Both antibonding states coincide in the energy interval. They broaden and shift to lower values when the molecule is at the gold surface (from 4−7 eV to 2−6 eV). The separation between the highest occupied bonding states (HOMO) and the lowest unoccupied antibonding states (LUMO) for S−H in the molecule is about 7 eV. According to the model discussed above, this difference corresponds to -2β, giving a bonding energy of about 3.5 eV, which is in agreement with experimental values[51] and previous theoretical calculations.[6] This energy difference HOMO−LUMO seems to be the same for the molecule at the gold surface.

In the following, we analyze the changes on the electronic states during the S−H bond breaking. As described above, the position of the S atom was frozen in the *xy* plane, keeping the atom free to relax in the *z* direction for a series of S−H distances. Figure 5 shows the electronic structure for increasing elongations of the S−H bond. The corresponding DOS for a molecule far away from the gold surface is shown in the inset for comparison. The groups of bonding and antibonding states of the S−H bond approach each other due to the decrease of the bond energy (-2β), as described by the theoretical model discussed above. In contrast, the energy gap between bonding and antibonding states for the C−S states remains constant because this bond is preserved during the dissociation of the S−H bond. However, these C−S states appear disturbed by the

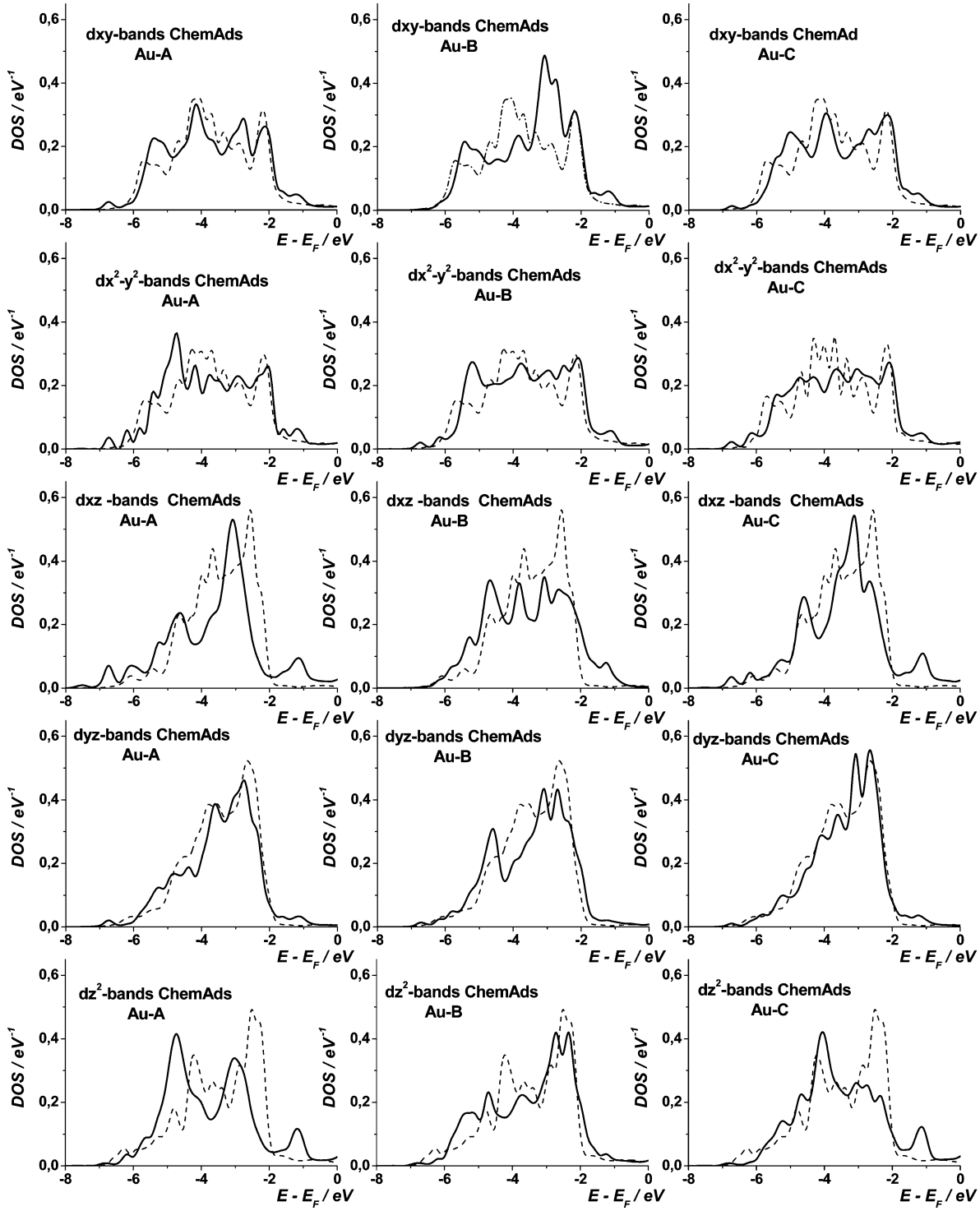

Figure 7. Projected DOS on the different components of the d bands for the three different gold atoms called A, B, and C, for the gold surfaces covered by the chemisorbed species shown in Figure 2-middle. The corresponding electronic states in the absence of adsorbate (dotted lines) are also shown for comparison.

indirect effect mentioned above for tuning the through-bond interaction. In the case of the molecule approaching the surface, at an elongation of the S−H bond of 2.13 Å the antibonding states begin to cross the Fermi level and start to be partially occupied, weakening the bond. Finally, at an S−H separation of 2.29 Å, the bond is broken and the hydrogen becomes adsorbed at the gold surface. The final separation between sulfur and hydrogen is 2.76 Å. Bonding and antibonding states appear, but now between the hydrogen and the gold surface. The sulfur states corresponding to the lone electron pairs slightly shift to higher energies, becoming partially unoccupied.

Nevertheless, the interaction of the sulfur atom with the gold surface is still weak at this S−H distance. This interaction becomes stronger only after allowing complete relaxation of the system, so that the hydrogen can desorb and the sulfur atom readjusts its geometry. It is also noticeable that the gold surface facilitates the S−H dissociation, since the isolated molecule cannot lose the hydrogen even for an elongation of the S−H bond of 2.29 Å, as can be observed in the insets. The bond is weakened, but the hydrogen atom is still attached to the sulfur. Figure 5 brings an additional information: the S levels are destabilized through chemical adsorption. This is due to the loss

of the covalent SH bond. This suggests that XPS S 2p binding energies would be lower in the case of dissociative adsorption than in the case of physisorption.

Figure 6 shows the electronic states for the final state, when the radical of the thiol is adsorbed at the gold surface and the hydrogen is desorbed. One can observe that due to the shorter distance between the sulfur and the gold atoms of the surface, the interaction is stronger compared with that of the "PhysAds" species discussed in the beginning of this section, leading to the broadening of the electronic states. The DOS projected on the carbon atom of the C−S states is again indirectly affected, although the broadening is still less than that of the sulfur atom. To compare this effect with the electronic states of the isolated radical, in this case calculations taking into account the spin polarization must be performed, since the number of electrons is odd. The results are shown in the inset of the Figure 6. The polarization is especially important for the states between −2 and +1 eV corresponding to the lone pair electrons of the sulfur. These states have been also observed for the adsorption of the radical of cysteine on Au (111).[16,17] Supported by an analysis of the one-particle electron states, Di Felice et al.[16,17] have assigned the states between −2 and −1 to bonding states and those above −1 eV to antibonding states between the sulfur and the d band of gold.

d. Interactions with the d Bands. The interaction of the different components of the d-band of gold with the s−p orbitals of sulfur and the s orbital of hydrogen changes for the different geometrical structures. It is well-known that a set of three different d orbitals can be distinguished for the surface of the slab in the absence of any adsorbate: the components projected on the plane of the surface (d_{xy} and $d_{x^2-y^2}$), at 45° of the surface (d_{xz} and d_{yz}), and perpendicular to it (d_{z^2}). When an adsorbate is present at the interface, the symmetry is broken and all the components are different. There are two different effects: On one hand, gold atoms of the surface are displaced from their equilibrium positions when the adsorbate is present and thus the overlapping with the orbitals of the neighbor gold atoms is affected. On the other hand, there exists the possibility of formation of localized bonds between the gold atoms and those of the adsorbate. In our case, these effects are clearly observed for the chemisorbed species and especially for the nearest gold atom (Au-A). Figure 7 shows the different components of the d-bands corresponding to the projection on the gold atoms called "A", "B", and "C". The d-bands of the surface atoms of the slab without the adsorbate are also shown for comparison. One can notice the modifications observed between −4.5 and −2.5 eV on the d_{xy} component projected at the atom "B". Although this atom is the most distant from the sulfur atom and the least displaced from the original position before the adsorption (see Figure 2b), it shows a lower coordination than the atoms "A" and "C". Effectively, the latter atoms are displaced together out of the original xy-plane and they consequently have a larger overlap of their orbitals. A new peak appears between −2 eV and the Fermi level at the d_{xz} and d_{z^2} components for all atoms with exception of the d_{z^2} corresponding to atom "B". This can correspond to the formation of a bond between the lone pair of the sulfur and the d-orbitals of gold (compare with the s−p orbitals of the sulfur atom shown in Figure 6). In the case of the adsorbed species still containing the hydrogen ("PhysAds") the s−p orbitals of the lone pair are shifted to lower energies in agreement with the shift of this new peak of the d bands. Following the evolution of the s−p orbitals during the S−H bond breaking, it could be possible that antibonding Au−S states emerge around the Fermi level. However, more detailed calculations are necessary to confirm this statement. The component d_{z^2} seems to be totally different for the three gold atoms "A−B−C". Electronic states projected onto the atoms "A" and "C" (the closest to the sulfur atom) show important changes in comparison with those in the absence of adorbate. A decrease on the density of states between −3 and −2 eV and an increase at lower and higher energies are observed. It must be stressed that these atoms are farther from the second gold layer and consequently they also have a lower possibility to overlap with the gold atoms of the under layer in comparison with the atom "B".

Conclusions

To understand the interactions of the alkanethiol adsorbate with the surface of Au(111), DFT calculations combined with a new theory for bond-breaking are performed, using propanethiol as the model system. The adsorption energetics shows that the adsorption process becomes less thermodynamically favorable with increasing surface coverage rate. The physisorption and chemisorption geometry and energetics are calculated and in comparison with the experiment. A theoretical potential energy surface for the thiol adsorption process is also presented. It is found that the chemisorption reaction occurs in two steps: A first one, where the breaking of the S-H bond occurs, with a barrier of about 0.32 eV followed by a spontaneous second step (barrier less), with the binding of the RS radical to the gold surface. The calculated energetics are in agreement with experimentally proposed values.

The projected density of states (DOS) projected on the different atoms of the systems has been calculated and the contributions of the different orbitals to the formation of bonds have been investigated. The d orbitals of gold with components perpendicular to the surface, especially the d_{z^2} and d_{xz} are involved in the formation of bonds with the thiols sulfur atom. The bonding and antibonding electronic states of the S−H bond have been identified and its evolution during the process of bond-breaking carefully analyzed. The corresponding bonding and antibonding states for the C−S bond are practically not affected during this process indicating that the bond is preserved. The s orbital of the hydrogen atom strongly interacts with the gold surface and finally a bond is formed. However, after total relaxation of the systems, the hydrogen atom desorbs.

A perturbation in the overlap between the gold atoms is also observed, because of the displacement of their positions relative to the surface in absence of adsorbate.

Acknowledgment. This work was performed using HPC resources from GENCI- [CCRT/CINES/IDRIS] (Grant 2009-[x2009082022]) and the CCRE of Université Pierre et Marie Curie. COST action D36, WG No D36/0006/06 and D36/0006/05, CONICET, DFG (Sa1770/1-1,2) and ELCAT are acknowledged for financial support. Dr. B. Diawara from LCPS ENS Paris is kindly acknowledged for providing us with *ModelView* used in the visualization of the structures.

References and Notes

(1) Schreiber, F. *Prog. Surf. Sci.* **2000**, *65*, 151.
(2) Schreiber, F. *J. Phys.: Condens. Matter* **2004**, *16*, R881.
(3) Love, J. C.; Estroff, L. A.; Kriebel, J. K.; Nuzzo, R. G.; Whitesides, G. M. *Chem. Rev.* **2005**, *105*, 1103.
(4) Whitesides, G. M.; B, G. *Science* **2002**, *295*, 2418.
(5) Lustemberg, P. G.; Martiarena, M. L.; Martínez, A. E.; Busnengo, H. F. *Langmuir* **2008**, *24*, 3274.
(6) Andreoni, W.; Curioni, A.; Grönbeck, H. *Int. J. Quantum Chem.* **2000**, *80*, 598.

(7) Rzeznicka, I. I.; Lee, J.; Maksymovych, P.; Yates, J. T., Jr. *J. Phys. Chem. B* **2005**, *209*, 15992.
(8) Kankate, L.; Turchanin, A.; Gölzhäuser, A. *Langmuir* **2009**, *25*, 10435.
(9) Zhou, J.-G.; Williams, Q. L.; Hagelberg, F. *Phys. Rev. B* **2007**, *76*, 075408.
(10) Ulman, A. *Chem. Rev.* **1996**, *96*, 1533.
(11) Vericat, C.; Vela, M. E.; Benitez, G. A.; Martin Gago, J. A.; Torrelles, X.; Salvarezza, R. C. *J. Phys.: Condens. Matter* **2006**, *18*, R867.
(12) Gonzalez-Lakunza, N.; Lorente, N.; Arnau, A. *J. Phys. Chem. C* **2007**, *111*, 12383.
(13) Rodriguez, J. A.; Dvorak, J.; Jirsak, T.; Liu, G.; Hrbek, J.; Aray, Y.; Gonzalez, G. *J. Am. Chem. Soc.* **2003**, *125*, 276.
(14) Yourdshahyan, Y.; Rappe, A. M. *J. Chem. Phys.* **2002**, *117*, 825.
(15) Santos, E.; Avalle, L.; Potting, K.; Velez, P.; Jones, H. *Electrochem. Acta* **2008**, *53*, 6807.
(16) Di Felice, R.; Selloni, A. *J. Chem. Phys.* **2004**, *120*, 4906.
(17) Di Felice, R.; Selloni, A.; Molinari, E. *J. Phys. Chem. B* **2003**, *107*, 1151.
(18) Hayashi, T.; Morikawa, Y.; Nozoye, H. *J. Chem. Phys.* **2001**, *114*, 7615.
(19) Gonzalez, N.; Lorente, N.; Arnau, A. *Surf. Sci.* **2002**, *600*, 4039.
(20) Cometto, F.; Paredes-Olivera, P.; Macagno, V.; Patrito, E. *J. Phys. Chem. B* **2005**, *109*, 21737.
(21) Masens, C.; Ford, M. J.; Cortie, M. B. *Surf. Sci.* **2005**, *580*, 19.
(22) de Bocarmé, T. V.; Chau, T.-D.; Tielens, F.; Andrés, J.; Gaspard, P.; Wang, L. R. C.; Kreuzer, H. J.; Kruse, N. *J. Chem. Phys.* **2006**, *125*, 054703.
(23) Santos, E.; Koper, M. T. M.; Schmickler, W. *Chem. Phys.* **2008**, *344*, 195.
(24) Santos, E.; Lundin, A.; Pötting, K.; Quaino, P.; Schmickler, W. *Phys. Rev. B* **2009**, *79*, 235436.
(25) Santos, E.; Schmickler, W. *Chem. Phys.* **2007**, *332*, 39.
(26) Tielens, F.; Humblot, V.; Pradier, C.-M. *Int. J. Quantum Chem.* **2008**, *108*, 1792.
(27) Tielens, F.; Humblot, V.; Pradier, C.-M.; Calatayud, M.; Illas, F. *Langmuir* **2009**, *25*, 9980.
(28) Doneux, T.; Tielens, F.; Geerlings, P.; Buess-Herman, C. *J. Phys. Chem. A* **2006**, *110*, 11346.
(29) Tielens, F.; Costa, D.; Humblot, V.; Pradier, C.-M. *J. Phys. Chem. C* **2008**, *112*, 182.
(30) Tielens, F.; Andrés, J.; Chau, T.-D.; de Bocarmé, T. V.; Kruse, N.; Geerlings, P. *Chem. Phys. Lett.* **2006**, *421*, 433.
(31) Tielens, F.; Andrés, J.; Van Brussel, M.; Buess-Herman, C.; Geerlings, P. *J. Phys. Chem. B* **2005**, *109*, 7624.
(32) Kresse, G.; Furthmuller, J. *Phys. Rev. B* **1996**, *54*, 11169.
(33) Kresse, G.; Joubert, J. *Phys. Rev. B* **1999**, *59*, 1758.
(34) Perdew, J. P.; Burke, K.; Ernzerhof, M. *Phys. Rev. Lett.* **1996**, *77*, 3865.
(35) Perdew, J. P.; Burke, K.; Ernzerhof, M. *Phys. Rev. Lett.* **1997**, *78*, 1396.
(36) Zhang, Y. K.; Yang, W. T. *Phys. Rev. Lett.* **1998**, *80*, 890.
(37) Perdew, J. P.; Burke, K.; M., E. *Phys. Rev. Lett.* **1996**, *77*, 3865.
(38) Blöchl, P. E.; Jepsen, O.; Andersen, O. K. *Phys. Rev. B* **1994**, *49*, 16223.
(39) Kresse, G.; Joubert, D. *Phys. Rev. B* **1999**, *59*, 1758.
(40) Anderson, P. W. *Phys. Rev.* **1961**, *124*, 41.
(41) Newns, D. M. *Phys. Rev.* **1969**, *178*, 1123.
(42) Levstein, P. R.; Pastawski, H. M.; D'Amato, J. L. *J. Condens. Matter.* **1990**, *2*, 1781.
(43) Pastawski, H. M.; Foa Torres, L. E. F.; Medina, E. *Chem. Phys.* **2002**, *281*, 257.
(44) Marcus, R. A. *J. Chem. Phys.* **1965**, *241*, 966.
(45) Hush, N. S. *J. Chem. Phys.* **1958**, *281*, 962.
(46) Vargas, M. C.; Selloni, A. *Rev. Mexicana Fis.* **2004**, *50*, 536.
(47) Lavrich, D. J.; Wetterer, S. M.; Bernasek, S. L.; Scoles, G. *J. Phys. Chem. B* **1998**, *102*, 3456.
(48) Cao, Y.; Ge, Q.; Dyer, D. J.; Wang, L. *J. Phys. Chem. B* **2003**, *107*, 3803.
(49) Gottschalck, J.; Hammer, B. *J. Phys. Chem.* **2002**, *116*, 784.
(50) Dubois, L.; Zegarski, B.; Nuzzo, R. *J. Chem. Phys.* **1993**, *98*, 678.
(51) Nicovic, J. M.; Kreutter, K. D.; van Dijk, C. A.; Wine, P. H. *J. Phys. Chem.* **1992**, *96*, 2518.
(52) Maksymovych, P.; Sorescu, D.; Yates, J. T., Jr. *J. Phys. Chem. B* **2006**, *110*, 21161.

JP102036R